

The rights and wrongs of rescaling in population genetics simulations

Parul Johri^{1,2,3,*}, Fanny Pouyet⁴ and Brian Charlesworth⁵

¹Department of Biology, The University of North Carolina at Chapel Hill, Chapel Hill, NC 27599, United States

²Department of Genetics, The University of North Carolina at Chapel Hill, Chapel Hill, NC 27599, United States

³Integrative Program for Biological and Genome Sciences, The University of North Carolina at Chapel Hill, Chapel Hill, NC 27599, United States

⁴Université Paris-Saclay, CNRS, Laboratoire Interdisciplinaire des Sciences du Numérique, Gif-sur-Yvette, France

⁵Institute of Ecology and Evolution, School of Biological Sciences, University of Edinburgh, Edinburgh EH9 3FL, United Kingdom

*To whom correspondence may be addressed at pjohri@unc.edu

Abstract

Computer simulations of complex population genetic models are an essential tool for making sense of the large-scale datasets of multiple genome sequences from a single species that are becoming increasingly available. A widely used approach for reducing computing time is to simulate populations that are much smaller than the natural populations that they are intended to represent, by using parameters such as selection coefficients and mutation rates, whose products with the population size correspond to those of the natural populations. This approach has come to be known as rescaling, and is justified by the theory of the genetics of finite populations.

Recently, however, there have been criticisms of this practice, which have brought to light situations in which it can lead to erroneous conclusions. This paper reviews the theoretical basis for rescaling, and relates it to current practice in population genetics simulations. It shows that some population genetic statistics are scaleable while others are not. Additionally, it shows that there are likely to be problems with rescaling when simulating large chromosomal regions, due to the non-linear relation between the physical distance between a pair of separate nucleotide

sites and the frequency of recombination between them. Other difficulties with rescaling can arise in connection with simulations of selection on complex traits, and with populations that reproduce partly by self-fertilization or asexual reproduction. A number of recommendations are made for good practice in relation to rescaling.

Keywords: diffusion equations, population genetics, recombination, rescaling, simulations

1. Introduction

Computer simulations of complex genetic models that include finite population size effects have a long history in population genetics, dating back to the late 1950s: for some early studies, see Fraser (1957); Fraser and Burnell (1970); Hill and Robertson (1966); Robertson (1970); Franklin and Lewontin (1970). With the advent of large-scale genome sequences from multiple individuals of the same species, computer simulations have become an essential tool for interpreting the data (e.g., Booker and Keightley 2018). A widely used approach for reducing computing time is to simulate populations that are much smaller than the natural population that they are designed to represent, an approach that has come to be known as rescaling (Comeron and Kreitman 2002; Hoggart et al. 2007). This is based on the principle that, provided that the assumptions of diffusion equation theory (discussed in section 2 below) are met, the evolution of a finite population is determined by the products of the variance effective population size (N_e) and the parameters that describe the intensity of the various evolutionary forces (selection coefficients, mutation rates, migration rates, recombination rates), rather than the absolute values of these parameters (for a detailed account of diffusion equations in populations, see Ewens (2004, Chapters 4 and 5). This principle was probably first explicitly formulated by Robertson (1960) in his seminal paper on the limits to a response to selection, who wrote that “The change in ϕ at a particular value of q in an amount of time t/N is dependent only on Ns and on the initial function $\phi(q, 0)$. It then follows that the pattern of the change is determined by Ns and its timescale is directly proportional to N .” Here, $\phi(q, t)$ is the probability density function for allele frequency q at time t , N is the effective population size, and s is the selection coefficient acting on a semi-dominant allele at the locus in question.

The widely used method of Monte Carlo simulations of a diploid Wright-Fisher population of size N assumes random sampling of gametes from the $2N$ haploid genomes of the

surviving adults in a given generation, assuming no distinction of sex among individuals (Ewens 2004, Chapter 1). If N for the simulated population is obtained by dividing the size of the corresponding natural population by a factor C ($C > 1$), and the deterministic parameters are multiplied by C , the outcome of the simulation with respect to many variables of interest should reflect the behavior of the natural population. As discussed below, such variables are either unaffected by the rescaling or have a known relationship with C , in which case the results from the simulation can be adjusted to match the natural population by using the appropriate transformation. The time taken to reach a given state of the population is expected to be divided by C as a result of rescaling, so that two major savings of computer time result from rescaling. The use of the coalescent process for simulating populations and inferring genetic parameters and demographic history similarly assumes that the products of effective population size and deterministic parameters are sufficient to describe the processes involved (Ewens 2004, Chapter 10; Wakeley 2008).

The general validity of rescaling has, however, recently been challenged (Dabi and Schrider 2025; Ferrari et al. 2025; Marsh et al. 2026), although studies have shown that rescaling does not affect most summary statistics of interest under neutrality (e.g., Adrián et al. 2020; Cury et al. 2022; Marsh et al. 2026). Our purpose here is to examine the population genetic justification for rescaling, to determine which evolutionary parameters are likely to be rescaleable and which are not, and to suggest guidelines for deciding on how to use rescaling.

2. The argument from diffusion equation theory

As the above quotation from Robertson (1960) shows, the logic of rescaling comes from the use of diffusion equations to model finite populations (Robertson 1960; Hill and Robertson 1966). These equations are, however, only approximations to the discrete generation processes that are the basis of most forward simulation methods. For example, in the case of a single autosomal diallelic locus in a Wright-Fisher population, the column vector $\mathbf{f}(t)$ of the probabilities $f_i(t)$ of finding i copies of allele A_2 and $2N - i$ copies of allele A_1 among a total of the $2N$ alleles present in breeding adults (where $i = 0, 1, \dots, 2N$) can always be related to $\mathbf{f}(t-1)$ by a matrix equation of the form $\mathbf{f}(t) = \mathbf{A} \mathbf{f}(t-1)$, where the elements of \mathbf{A} describe the probabilities of transition between the different frequencies as a result of the action of deterministic forces and the random sampling effects of finite population size (Ewens 2004, Chapter 1). The diffusion equation approximation

passes from a discrete time and discrete frequency representation to a continuous time and continuous frequency one (Ewens 2004, Chapters 1, 4, 5). This is justified if the changes in the components of f between generations are sufficiently small as to be effectively continuous, and if $2N$ is sufficiently large that allele frequencies are closely packed together on the closed interval $[0, 1]$. The discrete probability distribution f for allele frequency $q = i / (2N)$ between 0 and 1 is then replaced by a probability density function $\phi(q, q_0, t)$ (where q_0 is the initial value of q). If the moments of the change in q between generations are all negligible, apart from the expected change in q ($M_{\delta q}$) and the variance in the change in q ($V_{\delta q}$) the change in $\phi(q, q_0, t)$ per generation is described by the forward Kolmogorov equation (Ewens 2004, Chapter 4), which also requires that second- and higher-order terms in $M_{\delta q}$ be neglected. This means that $V_{\delta q} = pq/(2N_e)$, where $p = 1 - q$ and N_e is the variance effective population size (Crow 1954). The following version of the Kolmogorov forward equation then holds:

$$\frac{\partial \phi(q, q_0, t)}{\partial t} = \frac{1}{2N_e} \frac{\partial^2 (pq\phi)}{\partial q^2} - \frac{\partial (M_{\delta q}\phi)}{\partial q} \quad (1)$$

It is important to note that the need for small $M_{\delta q}$ does not necessarily require a variable such as the selection coefficient s in Equation (2) below to be small. For example, if q is confined to values close to zero, as would be the case for a strongly selected deleterious mutation, $M_{\delta q}^2$ would be negligible compared with $M_{\delta q}$ and $V_{\delta q}$. Diffusion equation results have, therefore, been successfully applied to problems such as the probability distribution of recessive lethal mutations in populations (Nei 1968). Similarly, in the case of a pair of autosomal loci with recombination frequency r in a randomly mating population, the expected change per generation in the coefficient of linkage disequilibrium due to recombination (D) is $M_{\delta D} = -rD$ (Robbins 1918). In eukaryote reproduction, r normally takes a maximum value of one-half, which applies both to a pair of loci on separate chromosomes and to a pair that are a long way apart on the same chromosome, provided that crossing over occurs at the four-strand stage of the first division of meiosis and that there is no chromatid interference. In theory, chromatid interference could give r values greater than one-half (Owen 1953) but there is little evidence for its occurrence except in some between-species hybrids in plants (Sarens et al. 2021). For most biologically realistic cases, a large value of r leads to small values of D unless the population

size is very small or selection favoring linkage disequilibrium is strong relative to r (Ewens 2004, Chapter 6). In this case, it can be assumed that $M_{\delta D}^2$ is negligible, so that diffusion theory can be used even for loosely linked pairs of loci. Similar principles apply to measures of linkage disequilibrium among multiple loci (Ewens 2004, Chapter 6).

Both sides of Equation (1) can be multiplied by $2N_e$, which is equivalent to measuring time in units of $2N_e$ generations, replacing $V_{\delta q}$ with $p(1 - p)$, and $M_{\delta q}$ with $2N_e M_{\delta q}$. If $M_{\delta q}$ can be written as the product of a constant and a function of q , the constant term is replaced by its product with $2N_e$. For example, the standard model of selection on an autosomal locus in a randomly mating population with selection coefficient s and dominance coefficient h (Ewens 2004, p.13), such that the relative fitnesses of A_1A_1 , A_1A_2 and A_2A_2 are 1, $1 + hs$ and $1 + s$, gives:

$$M_{\delta q} = spq[h + (1 - 2h)q] + O(s^2) \quad (2)$$

Provided that the terms in s^2 can be neglected, s can be replaced by $\gamma = 2N_e s$, and the properties of $\partial\phi(q, q_0, t)/\partial t$ are unchanged, except for the change in time-scale, provided that the initial condition q_0 is held constant. Note, however, that the dominance coefficient h is not to be rescaled, as it simply modulates the effect of s on $M_{\delta q}$. A similar principle applies to more general genetical situations, such as multiple loci, and to the backward Kolmogorov equation, which is used for solving problems such as the fixation probability of an allele and its expected sojourn time in the population (Ewens 2004, Chapters 4 and 5). Note, however, that fixation probabilities are proportional to C in rescaled populations (Table 1).

If the outcome of the process being studied is independent of the initial conditions, as is the case for the statistics of a stationary probability distribution, such as the moments of the allele frequency q or derived quantities like the genetic diversity as measured by the expectation of $2pq$, the values of these statistics are determined purely by the products of N_e with the parameters describing the changes per generation in allele or haplotype frequencies, provided that these can be written in a similar form to Equation (1).

This principle yields familiar results such as the inverse dependence of the extent of differentiation of neutral allele frequencies between local populations on $4N_e m$ (where m is the migration rate) in Wright's island model (Wright 1931), or that of the inverse dependence of the expected magnitude of linkage disequilibrium among a pair of neutral sites on $4N_e r$, where r is

the recombination frequency (Ohta and Kimura 1971). Such quantities would be completely unaffected by rescaling to a different population size, provided that the assumptions of diffusion equation theory are met and the products of the deterministic parameters with N_e are held constant. The same applies to properties that depend (to a good level of approximation) on the ratios of deterministic parameters, such as the ratio u/s in deterministic models of mutation selection balance or r/s in models of background selection and selective sweeps (Charlesworth and Jensen 2021). Similarly, properties such as the genetic load that are linear functions of s for a given set of genotype frequencies (Crow 1970), are to be scaled by a factor of C in the reduced population, assuming that the genotype frequencies are unaltered by the rescaling, and properties that are quadratic functions of s (such as the genetic variance in fitness) are to be scaled by C^2 , so that it is easy to transform simulated values to those for the natural population.

There is, however, a problem with properties that depend on the initial conditions, such as the initial frequencies of new mutations. These cannot be held constant if the population size N in a simulation is rescaled by dividing N by a factor of $C \gg 1$ and the deterministic parameters such as s are multiplied by C , compared with the natural population that is being simulated. It is thus important to examine the conditions under which this problem is likely to affect the outcome of a rescaled simulation. The type of approach involved can be illustrated by the simple case of the rate of substitution, K , of new mutations under positive or negative selection in a Wright-Fisher population with N breeding individuals, assuming that substitutions at different sites in the genome occur independently of each other. The mathematical details are presented in the Appendix (section 1) and summarized in Table 1. In this case, K is equal to the product of the rate of input of new mutations ($2Nu$) and their probability of fixation, denoted here by $Q(q_0)$, where $q_0 = 1/N_H$ in the case of a new mutation (Kimura and Ohta 1971, Chapter 1); N_H is the number of haploid genomes among breeding adults ($N_H = 2N$ in the case of an autosomal locus).

The conclusion from the results presented in section 1 of Appendix is that we can use simulations of a small population to predict the rates of substitution in a large population, provided that the selection coefficient in the reduced population (Cs , where s is the selection coefficient for the unscaled population) is sufficiently small that second-order terms in Cs can be neglected. This condition on Cs poses severe limitations on what strength of selection can realistically be modeled; for example, a selection coefficient of -0.1 for a deleterious mutation in the natural population would turn into a meaningless value of -10 if $C = 100$. This problem with

the magnitude of s will, of course, be encountered in all types of situations involving selection, such as temporally fluctuating selection, background selection, Hill-Robertson interference, and selective sweeps (Charlesworth and Jensen 2021).

Other features of interest may, however, be sensitive to initial conditions; for example, section 2 of the Appendix shows that the expected time to loss of a mutation (conditioned on loss) in a population of constant size is a function of $\ln(N_H)$ and hence is not scaleable; this is not, however, the case for the expected conditional time to fixation, which is scaleable. Since the expected number of segregating mutations under the infinite sites model (Ewens 2004, Chapter 9) is a function of the net expected time to loss or fixation of mutations, it is also a function of $\ln(N_H)$ and cannot be rescaled.

In contrast, the site frequency spectrum of segregating mutations in a sample from the population is scaleable (section 3 of the Appendix). The same applies to the effects of selective sweeps on neutral diversity under quite general single-locus selection models, provided that $N_{es} \gg 1$; population size affects the results only through N_{es} and N_{er} , at least to a good level of approximation (Charlesworth 2020a; Charlesworth 2020b; Cury et al. 2022). Table 1 describes the scalability properties of a number of quantities of interest to population geneticists.

3. Effects of rescaling on different simulation methods

One class of simulation method is to combine the deterministic recursion relations for a given genetic system with a random sampling scheme, either by means of the matrix representation of the probability distribution described above (e.g., Eyre-Walker and Keightley 2009), or by use of random numbers to simulate sampling from the genotype frequencies generated from the deterministic recursion for a single generation to obtain the transition to the next generation (e.g., Olioto and Abbott 2025).

A related procedure is the PoMo (Polymorphism- Aware Phylogenetic Model) method of jointly analysing within- and between-species multiple sequences (De Maio et al. 2013; Schrempf et al. 2019). This uses a single-locus, Moran population genetics model based on the birth-death process (Ewens 2004, pp.104-109) rather than a Wright-Fisher model, with a small haploid virtual population size that allows rapid computations of the desired statistics, especially phylogenetic tree properties. It can include certain types of selection and biased gene conversion as well as mutation and drift (Borges et al. 2022).

Another class involves forward-in-time individual-based simulations, including the popular *SLiM* simulation package (Hernandez 2008; Thornton 2014; Hernandez and Uricchio 2015; Haller and Messer 2019). For example, when simulating a diploid population with no distinction of sex with a Wright-Fisher model of drift, new individuals are generated by randomly sampling pairs of gametes from N adults. These are exposed to selection, mutation, recombination etc. to produce the next generation of N adults.

With all of these methods, other than the PoMo procedure, the size of the population that can be modeled is necessarily limited, either because of the difficulty of computing with large matrices, or because of the time needed to produce N adults, although recent developments have extended computations to larger population sizes and selection coefficients (Spence et al. 2023).

A third class of method involves the use of backward-in-time coalescent process simulations (Wakeley 2008), which are now being applied to whole chromosomes or genomes by means of various algorithms that represent recombination events (Kelleher et al. 2016; Nelson et al. 2020; Baumdicker et al. 2022). These methods are computationally efficient, as only the sampled genomes are simulated, and the coalescent process inherently includes the rescaling of population size and recombination. However, for large sample sizes or very long genomic regions, the standard coalescent approximation may create biases in genealogical correlations, identity-by-descent, and long-range linkage disequilibrium, although they have now been correctly implemented in *msprime* using a combination of the Wright-Fisher and coalescent models (Nelson et al. 2020).

We therefore focus most of our attention on forward simulations. We first consider the most severe problem with rescaling, the rescaling of the rate of recombination.

4. The problem with recombination

The difficulty with rescaling the recombination rate arises from the following considerations. Given that the rate of crossing over between two loci, denoted here by r , is restricted to $0 \leq r \leq \frac{1}{2}$ for most eukaryotes by the rules of genetics, it would seem to be impossible to multiply r by C for loosely linked or unlinked pairs of loci if we then get $rC > \frac{1}{2}$. This is, however, not necessarily a difficulty for the first class of simulation methods described above, where the transition between generations for a pair of loci involves $M_{\delta D} = -rD$, which can be small even if r is arbitrarily large. Since it is $N_e r$ not r that matters for the corresponding diffusion equation

process, the biological limitation on r is unimportant, and there is no difficulty in applying rescaling to r , provided that only pairwise associations between loci need to be considered. The same applies to methods based on the coalescent process.

Modeling sex differences in recombination should not pose extra problems for rescaling. Basic theory on LD (Ewens 2004, Chapter 6) suggests that, for autosomes, a simple mean of male and female recombination rates can be used in simulations where the sexes of individuals are ignored; in the extreme case of no recombination in one sex, r calculated from the genetic map in the sex with recombination is simply weighted by $\frac{1}{2}$ for autosomes. For the X or Z chromosomes in species with degenerate Y or W chromosomes, weights of $\frac{2}{3}$ and $\frac{1}{3}$ for the r values in the homogametic and heterogametic sexes, respectively, should be used (Langley et al. 1988).

There is, however, a serious difficulty for individual-based simulation methods that attempt to represent whole genomes or whole chromosomes. These use random number generators to determine the number and location of crossover events on a chromosome. Most commonly, the phenomenon of crossover interference (Otto and Payseur 2019) is ignored. This allows the number of crossovers between a pair of homologous chromosomes to be selected from a Poisson distribution, and their locations to be assigned by random placement on the chromosome pair. In principle there is no limitation to the number of such crossovers. However, the effect of multiple crossovers is to cause r to increase less than linearly with the map distance d between a pair of loci (in Morgans); for the case of no crossover interference, Haldane's mapping function $r = \frac{1}{2}[1 - \exp(-2d)]$ applies (Haldane 1919). It follows that, if we rescale d to dC , r is always rescaled by a factor less than C , which approaches 1 as d increases. If other parameters, such as selection coefficients and mutation rates, are rescaled by C , rescaling introduces a disproportionality between the rate of crossing over and the other deterministic parameters, as well as with drift, compared with the natural population being simulated. Properties such as the effects of hitchhiking that depend on r/s , or randomly generated LD for neutral variants (which depends on N_{er}), or the extent of interference between selected alleles (which depends on s/r), will behave incorrectly in the simulations if d not r is rescaled by C , as can be seen in the simulations by Marsh et al. (2026). This is bound to affect the outcome of the evolutionary process if multiple loci along a chromosome are being simulated, where it is impossible to rescale each pair of crossover rates by the same C . A similar problem applies to

recombination between loci on different chromosomes; r for this case is necessarily one-half in a simulation, regardless of N , if the process of independent assortment of chromosomes is simulated for each individual in the population.

Complications also arise when using ancestral recombination graph (ARG) methods such as *Relate* (Speidel et al. 2019; Speidel et al. 2021), *tsinfer+tsdate* (Kelleher et al. 2019; Wohns et al. 2022), *ARGweaver* (Rasmussen et al. 2014) or *Singer* (Deng et al. 2024). These methods, which reconstruct local trees, rely on the distribution of recombination events along the chromosome and, importantly, on the resulting correlations between local genealogies. In methods that use the coalescent process with recombination, such as *ARGweaver* and *Singer*, breakpoints are generated by a Poisson process whose rate depends on the recombination rate per nucleotide site, while in *tsinfer* or *Relate*, breakpoints are approximated via the Li & Stephens (Li and Stephens 2003) method that uses hidden Markov process representation of recombination. Rescaling recombination rates can reduce the correlation between inferred and true local trees, as these methods only modify tree topology incrementally, but this does not hold true when the rescaled recombination rate parameter is too large. This can introduce biases into any analysis that relies on ARG topology, including selection, recombination or demographic inference.

There thus seem to be insuperable difficulties in simulating interactions between selection, mutation, recombination and drift that involve whole chromosomes or whole genomes if rescaling is required (Marsh et al. 2026), unless crossing over is rare or absent. For example, in a region under strong background selection, if N , s , and r are all rescaled proportionally, the ratio s/r at linked neutral sites is expected to be preserved, allowing neutral diversity to reflect the natural population accurately; however, in the presence of multiple crossovers, even proportional rescaling cannot prevent exaggerated reductions in diversity. As shown in Figure 1, the effect of background selection in reducing diversity matches theoretical expectations for small rescaling factors ($C = 100$ and 200), where only a single and a double crossover is expected per chromosome per generation, but is substantially exaggerated when higher rescaling factors ($C = 500$ and 1000) result in multiple crossovers (5 and 10 crossovers per chromosome per generation, respectively).

Probably the best that can be done is to simulate regions that are sufficiently short such that r is nearly linearly related to d after rescaling. This approach is facilitated by crossover

interference, whereby the occurrence of a crossover in a bivalent at meiosis I inhibits the occurrence of another crossover nearby (Otto and Payseur 2019; Girard et al. 2023). Interference reduces the frequency of multiple crossover events, causing the mapping function to become closer to linear. It is feasible to include interference in simulation methods, and this has been done in a study of identity by descent among relatives (Caballero et al. 2019), using an extension of the counting model of Foss et al. (1993). This model assumes that the sites of the initiation of recombination events are distributed randomly along a bivalent at the four-strand stage of meiosis, with a fixed number (m) of non-crossover (gene conversion) events separating two successive crossovers, and assuming no interference between sister chromatids. This process generates a gamma distribution of the map distance between successive crossovers in a bivalent, conditioned on a given rate of formation of points of initiation of recombination events, with the scale and shape parameters of the distribution both equal to $m + 1$. Writing $y = 2(m + 1)d$, the mapping function becomes:

$$r = \frac{1}{2}[1 - e^{-y} \sum_{i=0}^m \frac{y^i}{i!} \left(1 - \frac{i}{m+1}\right)] \quad (3)$$

Figure 2 shows the relation between r and d for several values of m , with $m = 0$ corresponding to the Haldane mapping function. It also shows the linear relation between r and d that results from the case of one crossover per bivalent with complete interference. This mapping function allows an estimate of the maximum length of a chromosome over which an approximately linear relation between r and d holds after rescaling d by a factor of C . If the map length of the chromosome in question is L and the interference parameter is m , the graph of Equation (3) allows visual determination of the value of d at which a significant departure from linearity is manifest, denoted by d_0 . The corresponding proportion of the chromosome is d_0/L . For the case of no interference, Figure 2 suggests that $d_0 = 0.35$ is a fairly liberal value. With $m = 10$, and 4, the corresponding values are 0.45 and 0.40, respectively. The rescaled value of the maximum permitted d , d_1 , must satisfy $d_1 = d_0/C$, and the corresponding proportion of the whole chromosome that can be simulated is thus $d_0/(CL)$. If the physical size of the chromosome is M megabases, the corresponding size of a permissible rescaled sequence is $Mc = d_0M/(CL)$. The procedure is simpler in the case of one obligate crossover per bivalent, which is close to what is observed in *C. elegans* (Hillers et al. 2017). Here, the rescaled maximum permissible map

distance is the same as the map length of the whole chromosome (0.5), and the maximum size of a rescaled sequence is simply M/C .

The extent of interference is highly variable among species (Otto and Payseur 2019; Ernst et al. 2024), so that the parameters to be used in a simulation where interference is modeled need to be chosen in relation to what is known about the organism in question. Table 2 provides some examples of species with different levels of interference, with corresponding recommendations for the permissible sizes of sequences after rescaling based on the above considerations. These examples are intended only as a very rough guide, as they ignore complexities such as the existence of sex differences in recombination rates, recombination hotspots, regional variation in the rate of crossing over along chromosomes (with greatly reduced rates near telomeres and centromeres being commonly observed), as well as the existence of two pathways to crossing over, only one of which is subject to interference (Copenhaver et al. 2002).

In *D. melanogaster*, for example, interference is nearly complete over 10cM of the standard female genetic map (Ashburner et al. 2005, Chapter 10), which corresponds approximately to four megabases of DNA and contains an average of roughly 500 genes. Without rescaling, a region of this size could be modeled by dropping a single crossover onto a pair of chromosomes with probability 0.1 in females, or a net probability of 0.05 if the absence of crossing over in males is taken into account. However, rescaling of such a region without allowing multiple events would be restricted to a C of 20, giving a probability of one for a crossover event. To rescale by a factor of 1000, which is often used in simulations of *Drosophila* populations (e.g., Johri and Charlesworth 2025), the size of the region corresponding to the same probability of a crossover would have to be reduced by a factor of 50, *i.e.*, to 80kb, enough to accommodate about eleven typical sized genes. In other words, the larger the rescaling factor, the shorter the size of the region that can be simulated accurately. In contrast, for simulations of human populations, with their much smaller N_e , a C value of 10 is quite feasible, so that a 100-fold larger region could be simulated without much loss of accuracy. This advantage is, of course, offset by the low gene density in humans, which means that only 10 typical genes could be accommodated in such a region.

Crossover interference is not currently directly modelled in *SLiM* and other popular population genetics simulation packages. The implementation of crossover interference in simulations is not straightforward (Caballero 2019), especially if one wants to incorporate

recombination rate heterogeneity across the genome as well as the existence of two crossover pathways. However, modeling crossover interference allows for more accurate simulations of whole chromosomes, and should probably be taken into account in future investigations.

Gene conversion is much less problematical in relation to scaling. It plays an important role in recombination over short distances, as gene conversion tracts in most organisms usually extend over a few hundred basepairs at most, *e.g.* 300-459 bp in humans (Williams et al. 2015; Masaki and Browning 2025) and ~440 bp in *D. melanogaster* (Comeron et al. 2012). It can be modelled by assigning a rate of initiation of a conversion tract, of similar magnitude to the rate of crossing over per basepair, together with an exponentially distributed tract length, such that the rate of recombination between two sites separated by z nucleotides is $2r_g d_g [1 - \exp(-z/d_g)]$, where r_g is the rate of occurrence of gene conversion events and d_g is the mean length of a tract (Frisse et al. 2001). If the physical organisation of the genome is retained in the simulations, then d_g should be kept constant while r_g is multiplied by C .

Many older simulation studies of multi-locus systems assumed that selection coefficients are sufficiently large that the evolutionary processes involved are deterministic, in which case relatively small population sizes can be simulated (*e.g.*, Charlesworth et al. 1992). The level of realism of these studies may, however, be questioned in the light of evidence for small Nes values for most deleterious mutations from natural populations (*e.g.*, Kim et al. 2017; Johri et al. 2020). The issue of scaling does not, of course, arise in simulations of natural populations with sufficiently small sizes that running time is not a problem, as in studies of problems in conservation genetics (*e.g.*, Robinson et al. 2022). The problems with modeling recombination noted above mean, however, that simulations of polygenic selection must encounter difficulties when large genomic regions are involved (discussed in section 5 below).

5. Selection on quantitative traits

Up to now, we have only considered population genetics models that directly assign fitnesses to genotypes. There is, however, considerable interest in the evolutionary dynamics of quantitative traits, where the dynamics of the variants at the individual loci that underly variation in the trait reflect the functional relation between trait and fitness, as well as the relations between the effects of the individual loci and the trait itself (Bulmer 1980; Bürger 2000; Walsh and Lynch 2018; Stephan and John 2020). Most recent simulation studies of selection on quantitative traits

do not use rescaling (e.g., Thornton 2019; Schaal et al. 2022), with the exception of Hartfield and Glémin (2024), which also involves the complication of partial self-fertilization (see below).

Given the current interest in modeling polygenic adaptation (Stephan and John 2020), the question arise of how to rescale the parameters involved in future simulation studies. We discuss this problem using the familiar nor-optimal or Gaussian fitness model of selection on a single continuously varying trait (Stephan and John 2020), whose phenotypic value is denoted here by z . The following expression represents the fitness of an individual with trait value z :

$$w(z) = \exp \left[-\frac{(z-z_0)^2}{2V_s} \right] \quad (3)$$

where z_0 is the optimal value of the trait and V_s is an inverse measure of the strength of selection on the trait, such that smaller values imply a faster decline in fitness as the trait value departs from the optimum.

If each locus has only a small effect on the trait, the rate of change of allele frequency in a given generation in a randomly mating population is determined by the additive and dominance effects of the locus on the trait (a and d , respectively) together with the deviation of the trait mean \bar{z} from z_0 , the phenotypic variance in the trait (V_z), and V_s (see Equations A12-A19 of the Appendix). In general, these parameters depend in a complex way on the details of how all the loci concerned determine trait values (dominance, epistasis, allele frequencies, linkage disequilibrium, etc) and will change over time (Bulmer 1980; Bürger 2000; Walsh and Lynch 2018, Chapter 24). However, in the absence of epistasis and genotype-environment interactions with respect to z , the equations should provide a good approximation to what happens over a single generation.

It is shown in the Appendix that, provided that selection is relatively weak (specifically, $V_s \gg V_z$), the selection coefficient s at a given locus is inversely proportional to V_s , independently of the scale on which z is measured. This result suggests that the factor C by which s should be multiplied when rescaling N by a factor of C can be obtained by dividing V_s by C , while leaving the scale of z unchanged. This means that a and d for each locus are unaffected by the rescaling, whereas s is multiplied by C . However, this procedure tacitly assumes that the magnitude of V_s has a negligible effect on the properties of the distribution of z ,

which is not exact, due to the effect of selection in generating linkage disequilibrium (Bulmer 1980; Bürger 2000; Walsh and Lynch 2018, Chapter 24).

Similar considerations should apply to the generalization of Equation (3) for multivariate traits under selection (Walsh and Lynch 2018, Chapter 30), but we have not investigated this question in detail. Given that there are serious conditions on the region of parameter space in which the above conclusion about scaling is valid, and the potential effects of epistasis and genotype—environment interactions have been ignored, rescaling of simulations of selection on quantitative traits should probably be conducted with caution.

6. Self-fertilization and facultative sex

We now consider some problems that arise with mating systems other than conventional random mating. First, the properties of partially self-fertilizing populations have attracted a good deal of attention, due to their importance for the understanding of processes such as the evolution of outcrossing mechanisms in plants (Hartfield et al. 2017). The impact of recombination in populations reproducing by a mixture of selfing and outcrossing is very different from that in randomly mating, outcrossing populations, because (to a good level of approximation), the recursion relation for D is $M_{\delta q} = -(1 - F)rD$, where F is the inbreeding coefficient generated by the current frequency of zygotes produced by selfing versus outcrossing (Nordborg 1997) . Under strict neutrality, the equilibrium value of F is equal to $S/(2 - S)$, where S is the frequency with which zygotes are produced by self-fertilization (Pollak 1987). It follows that, if F is close to unity, even loci on separate chromosomes have small effective rates of recombination, given approximately by $(1 - F)r$. For the first and third types of simulation methods described above, rescaling should present few difficulties, if this transformation is used to represent the frequency of recombination between a pair of loci and only a single pair of loci is modeled.

For individual based simulation methods, however, there are similar problems to those described above (if S is kept constant and r is scaled), unless a heuristic approach of replacing recombination frequencies by $(1 - F)r$ is used, in which case F would have to be re-determined from genotype frequencies every generation (note that the rate of selfing, S , is not scaleable), since the neutral formula does not necessarily apply when there is selection. Furthermore, F is likely to vary across the genome if there are regional differences in recombination rates, and hence differences in the effects of selection at linked sites. This procedure could thus be

problematical, especially as it is unclear whether this heuristic applies to multi-locus linkage disequilibria. Tests of its accuracy based on simulations with different population sizes would be desirable.

Facultative sexual reproduction might be expected to have similar properties to selfing, in that episodes of asexual reproduction are associated with a lack of recombination. Two extreme classes of facultative sex can be envisaged. The first is when there is a constant frequency α of sexual reproduction each generation. The recursion relations for a given genetic system in such a case can be written down as a combination of equations for sexual reproduction (contributing a fraction α of the new zygotes) and asexual reproduction (contributing a fraction $1 - \alpha$) (e.g., Agrawal and Hartfield 2016). This can easily be carried over into any of the simulation methods described above. In the limit of purely asexual reproduction, as in the case of Y or W chromosomes or clonal organisms, the problem of rescaling the rate of recombination does not arise, but it still exists for individual based simulations when $\alpha > 0$, just as in the case of selfing (like S , α is not scaleable).

The extreme alternative to this model is when sexual reproduction is episodic, occurring in only a fraction α of generations, and involving every individual in the population. The simplest case is when α is fixed, so that the interval between sexual generations is $1/\alpha$, but variation in α can also be modelled (Ollivier et al. 2025). This mode of reproduction is characteristic of unicellular eukaryotes such as *Chlamydomonas* or *Saccharomyces*, as well as multicellular cyclical parthenogens like *Daphnia*. While simulating such a situation presents no problem in principle, it is unclear how to relate it to a diffusion process, given the abrupt transitions between sexual and asexual reproduction, and hence how to scale α .

A recent study of the effect of a single selective sweep on neutral diversity at linked sites in a diploid species found that, provided the mean of α is sufficiently large that several episodes of sex occur during a sweep, the effect of the sweep on nucleotide site diversity is well predicted by the results for a randomly mating population, substituting $r\alpha$ for r , where r is the frequency of recombination between a focal neutral site and the target of selection, $\alpha h + (1 - \alpha)$ for h , and $\alpha (1 - 2h)$ for $(1 - 2h)$ in Equation (2) (Ollivier et al. 2025). In this situation, $r\alpha$ and s can both be rescaled. However, when at most only one or two episodes of sex occur during the sweep to fixation of an asexual diploid clone that is heterozygous for a beneficial mutation, there is an

abrupt phase transition to a situation when diversity relative to the purely neutral case is bounded below by $2r(1 - r)$, with an additional term of approximately $1/(2N_e\alpha)$. The first term represents the fact that a full sweep requires the initial sweep to be followed by a sexual generation, allowing the production of individuals homozygous for the beneficial mutation. The probability that a pair of these inherits non-identical alleles at the neutral site is $2r(1 - r)$, explaining the first term; the second term represents the bulk of the expected increase in diversity during the sweep. In this situation, r is completely unscaleable, whereas α is scaleable. This illustrates how unexpected complexities can emerge with mating systems that differ from the standard of random mating.

7. Population size changes

With nonequilibrium demography modelled by distinct epochs with different population sizes, so that N_H is a specified function of time, denoted by $N_H(t)$, a rescaled value $N_H(t)/C$ can be used in a simulation. To maintain the rate of coalescence at neutral sites for the original population, the duration (τ) of an epoch would also need to be scaled by C , so that $\tau = N_H(t)/C$ generations are simulated for the epoch in question. On one hand, such scaling can be highly beneficial as it reduces both the number of breeding individuals and the simulation time, reducing the total computational cost. However, it has certain limitations, especially when the magnitude of change in population size is large and the number of breeding individuals in the population at any time becomes very small. In particular, with very small population sizes the assumptions of the diffusion approximation and its corollary, the Kingman coalescent, break down, with multiple merger coalescents becoming important. In the extreme of a strong population bottleneck in a dioecious species, it is not possible to simulate fewer than two breeding individuals, which poses an obvious limit on the size of C . Similarly, if the population experiences a size change for a short time period τ' , C must be limited to a value less than τ' so that at least one generation elapses at the altered population size. It should be possible to scale a simulated population using different scaling factors during different epochs, e.g. one could, in principle, unscale a population during the bottleneck. However, it is unclear whether the dynamics of linkage disequilibrium and multi-locus selection would be accurately represented if this is done. This question requires further investigation. Analytical and computational methods for dealing with the effects of variable population size for single-locus models on the estimation of the distribution of variant

frequencies under both selection and neutrality, and applications to demographic inference and estimation of the distribution of mutational effects on fitness have recently been developed (Živković et al. 2015)..

8. Epistasis

There are two ways in which epistasis enters into population genetic models. The first is epistasis at the level of fitness itself, in which the fitness of multilocus genotypes depart from the predictions from additive or multiplicative combinations of the effects of each locus on its own (Ewens 2004, Chapters 6 and 7). This could pose a problem for rescaling if the fitness differences among genotypes represented in the population after rescaling become so large that the assumption of small changes in allele or haplotype frequencies is violated, or negative fitness values are produced. But this is not substantially different from the problem with large fitness differences encountered in the absence of epistasis.

The other role of epistasis is at the level of the phenotype on which selection acts (Barton 2017). The above discussion of selection on quantitative traits suggests that rescaling should be carried out on the measure of the intensity of selection on the trait, without rescaling the trait, but the consequences of epistasis at the trait level for rescaling remain to be explored.

9. Recommendations

1. We strongly recommend that whenever possible, one should check with available theory whether their population genetic quantity or statistic of interest is preserved with scaling, or if it scales with the scaling factor in a known manner. In both of these cases, one can successfully obtain the unscaled quantity/statistic from rescaled simulations. However, if the quantity is not scaleable, it is best not to utilize it. Table 1 summarizes the scalability properties of many quantities of interest in population genetics.
2. When simulating multiple linked sites, it is important to decide the length of the region that is likely to preserve the evolutionary dynamics for the problem under investigation, according to the criteria we have outlined above.
3. For modeling quantitative traits with a non-optimal selection model, the inverse measure of the strength of selection (V_s) should be scaled, not the scale on which the trait is measured. The

problems with rescaling recombination rates (point 2) should also be considered in connection with quantitative traits.

4. For simulations of species reproducing by partial self-fertilization, the probability of selfing (S) should not be scaled, in contrast to other evolutionary parameters. The effect of the extent of inbreeding on the rate of recombination needs to be considered in deciding on what length of sequence can be modeled in multi-locus simulations (as per our second recommendation).
5. Similar properties apply to species reproducing with constant frequency α of sexual reproduction each generation; the case of diploid populations with episodes of sexual reproduction alternating with asexual reproduction is more complex, and requires special treatment if the frequency of sex is very low (see above).
6. When simulating a very strong bottleneck, or large magnitudes of changes in population size, it would be best to use different scaling factors to test the sensitivity of results to rescaling.
7. The same applies to simulations with selection if there is a danger that rescaling will introduce unrealistically low fitnesses of genotypes with large numbers of deleterious mutations. In simulations with selection, it should be possible to compare theoretical expectations of diversity at neutral alleles to simulated observations, and a mismatch is likely to indicate problems with rescaling. However, this approach is only useful when simulating scenarios where theoretical expectations can be calculated. Often highly complex models are simulated using forward simulations, where it may be difficult to obtain theoretical expectations. In such cases, it would be best to compare the statistics of interest obtained from simulations with different scaling factors.

ACKNOWLEDGEMENTS

PJ was supported by the National Institute of General Medical Sciences of the National Institutes of Health under award number R35GM154969. FP work was supported by the ANR-25-CE12-4245-01 RECAF.

REFERENCES

Adrion JR et al. 2020. A community-maintained standard library of population genetic models. *eLife*. 9:e54967. <https://doi.org/10.7554/eLife.54967>

Agrawal AF, Hartfield M. 2016. Coalescence with background and balancing selection in systems with bi- and uniparental reproduction: Contrasting partial asexuality and selfing. *Genetics*. 202:313–326. <https://doi.org/10.1534/genetics.115.181024>

Ashburner M, Golic KG, Hawley RS. 2005. *Drosophila. A Laboratory Handbook*. 2nd edn. Cold Spring Harbor Press, Cold Spring Harbor, NY.

Barton NH. 2017. How does epistasis influence the response to selection? *Heredity*. 118:96–109. <https://doi.org/10.1038/hdy.2016.109>

Baumdicker F et al. 2022. Efficient ancestry and mutation simulation with msprime 1.0. *Genetics*. 220(3):iyab229. <https://doi.org/10.1093/genetics/iyab229>

Booker TR, Keightley PD. 2018. Understanding the factors that shape patterns of nucleotide diversity in the house mouse genome. *Mol Biol Evol*. 35(12):2971–2988. <https://doi.org/10.1093/molbev/msy188>

Borges R, Boussau B, Szöllösi GJ, Kosiol C. 2022. Nucleotide usage biases distort inferences of the species tree. *Genome Biol Evol*. 14(1):evab290. <https://doi.org/10.1093/gbe/evab290>

Broman KW, Weber JL. 2000. Characterization of human crossover interference. *Am J Hum Genet*. 66(6):1911–1926. <https://doi.org/10.1086/302923>

Bulmer MG. 1980. *The Mathematical Theory of Quantitative Genetics*. Clarendon Press, Oxford.

Bürger R. 2000. *The Mathematical Theory of Selection, Recombination, and Mutation*. John Wiley & Sons, Chichester, UK.

Caballero M et al. 2019. Crossover interference and sex-specific genetic maps shape identical by descent sharing in close relatives. *PLOS Genet*. 15(12):e1007979. <https://doi.org/10.1371/journal.pgen.1007979>

Charlesworth B. 2020a. How long does it take to fix a favorable mutation, and why should we care? *Am Nat*. 195(5):753–771. <https://doi.org/10.1086/708187>

Charlesworth B. 2020b. How good are predictions of the effects of selective sweeps on levels of neutral diversity? *Genetics*. 216(4):1217–1238. <https://doi.org/10.1534/genetics.120.303734>

Charlesworth B. 2022. The effects of weak selection on neutral diversity at linked sites. *Genetics*. 221(1):iyac027. <https://doi.org/10.1093/genetics/iyac027>

Charlesworth B, Jensen JD. 2021. Effects of selection at linked sites on patterns of genetic variability. *Annu Rev Ecol Evol Syst*. 52:177–197. <https://doi.org/10.1146/annurev-ecolsys-010621-044528>

Charlesworth D, Morgan MT, Charlesworth B. 1992. The effect of linkage and population size on inbreeding depression due to mutational load. *Genet Res*. 59(1):49–61. <https://doi.org/10.1017/S0016672300030160>

Comeron JM, Kreitman M. 2002. Population, evolutionary and genomic consequences of interference selection. *Genetics*. 161:389–410. <https://doi.org/10.1093/genetics/161.1.389>

Comeron JM, Ratnappan R, Bailin S. 2012. The many landscapes of recombination in *Drosophila melanogaster*. *PLOS Genet*. 8(10):e1002905. <https://doi.org/10.1371/journal.pgen.1002905>

Copenhaver GP, Housworth EA, Stahl FW. 2002. Crossover interference in *Arabidopsis*. *Genetics*. 160(4):1631–1639. <https://doi.org/10.1093/genetics/160.4.1631>

Cox A et al. 2009. A new standard genetic map for the laboratory mouse. *Genetics*. 182(4):1335–1344. <https://doi.org/10.1534/genetics.109.105486>

Crow JF. 1954. Breeding structure of populations. II. Effective population number. In: *Statistics and Mathematics in Biology*. eds. Kempthorne O, Bancroft TA, Gowen JW, Lush JL. Iowa State University Press, Ames, IA; p 543–556

Crow JF. 1970. Genetic loads and the cost of natural selection. In: Kojima K, editor. *Mathematical Topics in Population Genetics*. Springer-Verlag, Berlin; p 128–177 https://doi.org/10.1007/978-3-642-46244-3_5

Cury J, Haller BC, Achaz G, Jay F. 2022. Simulation of bacterial populations with SLiM. *Peer Community J*. 2:e7. <https://doi.org/10.24072/pcjournal.72>

Dabi A, Schrider DR. 2025. Population size rescaling significantly biases outcomes of forward-in-time population genetic simulations. *Genetics*. 229(1):iyae180. <https://doi.org/10.1093/genetics/iyae180>

De Boer E et al. 2006. Two levels of interference in mouse meiotic recombination. *Proc Natl Acad Sci*. 103(25):9607–9612. <https://doi.org/10.1073/pnas.0600418103>

De Maio N, Schlötterer C, Kosiol C. 2013. Linking great apes genome evolution across time scales using polymorphism-aware phylogenetic models. *Mol Biol Evol*. 30(10):2249–2262. <https://doi.org/10.1093/molbev/mst131>

Deng Y, Nielsen R, Song YS. 2024. Robust and accurate Bayesian inference of genome-wide genealogies for large samples. 2024.03.16.585351 [accessed 2025 Nov 26]. <https://www.biorxiv.org/content/10.1101/2024.03.16.585351v1>. <https://doi.org/10.1101/2024.03.16.585351>

Ernst M, Mercier R, Zwicker D. 2024. Interference length reveals regularity of crossover placement across species. *Nat Commun*. 15(1):8973. <https://doi.org/10.1038/s41467-024-53054-2>

Ewens WJ. 2004. *Mathematical Population Genetics 1: Theoretical Introduction*. Springer, New York, NY.

Eyre-Walker A, Keightley PD. 2009. Estimating the rate of adaptive molecular evolution in the presence of slightly deleterious mutations and population size change. *Mol Biol Evol*. 26(9):2097–2108. <https://doi.org/10.1093/molbev/msp119>

Ferrari T, Feng S, Zhang X, Mooney J. 2025. Parameter scaling in population genetics simulations may introduce unintended background selection: Considerations for scaled simulation design. *Genome Biol Evol*. 17(6):evaf097. <https://doi.org/10.1093/gbe/evaf097>

Fisher RA. 1930. The genetical theory of natural selection. Clarendon Press, Oxford.

Foss E, Lande R, Stahl FW, Steinberg CM. 1993. Chiasma interference as a function of genetic distance. *Genetics*. 133(3):681–691. <https://doi.org/10.1093/genetics/133.3.681>

Franklin I, Lewontin RC. 1970. Is the gene the unit of selection? *Genetics*. 65(4):707–734. <https://doi.org/10.1093/genetics/65.4.707>

Fraser A. 1957. Simulation of genetic systems by automatic digital computers I. Introduction. *Aust J Biol Sci*. 10(4):484–491. <https://doi.org/10.1071/BI9570484>

Fraser AS, Burnell D. 1970. Computer Models in Genetics. McGraw-Hill, New York, NY.

Frisse L et al. 2001. Gene conversion and different population histories may explain the contrast between polymorphism and linkage disequilibrium levels. *Am J Hum Genet*. 69(4):831–843. <https://doi.org/10.1086/323612>

Girard C, Zwicker D, Mercier R. 2023. The regulation of meiotic crossover distribution: a coarse solution to a century-old mystery? *Biochem Soc Trans*. 51(3):1179–1190. <https://doi.org/10.1042/BST20221329>

Haldane JBS. 1919. The combination of linkage values and the calculation of distance between loci of linked factors. *J Genet*. 8:299–309

Haldane JBS. 1930. A mathematical theory of natural and artificial selection. Part VII. Selection intensity as a function of mortality rate. *Math Proc Camb Philos Soc*. 27:131–136. <https://doi.org/10.1017/S0305004100009427>

Haldane JBS. 1937. The effect of variation on fitness. *Am Nat*. 71:337–349. <https://doi.org/10.1086/280722>

Haller BC, Messer PW. 2019. SLiM 3: Forward genetic simulations beyond the Wright–Fisher model. *Mol Biol Evol*. 36(3):632–637. <https://doi.org/10.1093/molbev/msy228>

Hartfield M, Bataillon T, Glémén S. 2017. The evolutionary interplay between adaptation and self-fertilization. *Trends Genet TIG*. 33(6):420–431. <https://doi.org/10.1016/j.tig.2017.04.002>

Hartfield M, Glémén S. 2024. Polygenic selection to a changing optimum under self-fertilisation. *PLOS Genet*. 20(7):e1011312. <https://doi.org/10.1371/journal.pgen.1011312>

Hernandez RD. 2008. A flexible forward simulator for populations subject to selection and demography. *Bioinformatics*. 24(23):2786–2787. <https://doi.org/10.1093/bioinformatics/btn522>

Hernandez RD, Uricchio LH. 2015. SFS_CODE: More efficient and flexible forward simulations. 025064 [accessed 2025 Oct 29]. <https://www.biorxiv.org/content/10.1101/025064v1>. <https://doi.org/10.1101/025064>

Hill WG, Robertson A. 1966. The effect of linkage on limits to artificial selection. *Genet Res.* 8(3):269–294

Hillers KJ, Jantsch V, Martinez-Perez E, Yanowitz JL. 2017. Meiosis. In: WormBook, eds. Villeneuve A, Greenstein D. The *C. elegans* Research Community; p 1–43 [accessed 2025 Dec 17]. <https://www.ncbi.nlm.nih.gov/books/NBK430708/>

Hoggart CJ et al. 2007. Sequence-level population simulations over large genomic regions. *Genetics*. 177(3):1725–1731. <https://doi.org/10.1534/genetics.106.069088>

Johri P et al. 2021. Revisiting the notion of deleterious sweeps. *Genetics*. 219(3):iyab094. <https://doi.org/10.1093/genetics/iyab094>

Johri P, Charlesworth B. 2025. A gene-based model of fitness and its implications for genetic variation: Linkage disequilibrium. *Genetics*. 231(3):iyaf168. <https://doi.org/10.1093/genetics/iyaf168>

Johri P, Charlesworth B, Jensen JD. 2020. Toward an evolutionarily appropriate null model: jointly inferring demography and purifying selection. *Genetics*. 215(1):173–192. <https://doi.org/10.1534/genetics.119.303002>

Kelleher J et al. 2019. Inferring whole-genome histories in large population datasets. *Nat Genet*. 51(9):1330–1338. <https://doi.org/10.1038/s41588-019-0483-y>

Kelleher J, Etheridge AM, McVean G. 2016. Efficient coalescent simulation and genealogical analysis for large sample sizes. *PLOS Comput Biol*. 12(5):e1004842. <https://doi.org/10.1371/journal.pcbi.1004842>

Kim BY, Huber CD, Lohmueller KE. 2017. Inference of the distribution of selection coefficients for new nonsynonymous mutations using large samples. *Genetics*. 206(1):345–361. <https://doi.org/10.1534/genetics.116.197145>

Kimura M. 1964. Diffusion models in population genetics. *J Appl Probab*. 1(2):177–232. <https://doi.org/10.2307/3211856>

Kimura M. 1971. Theoretical foundation of population genetics at the molecular level. *Theor Popul Biol*. 2(2):174–208. [https://doi.org/10.1016/0040-5809\(71\)90014-1](https://doi.org/10.1016/0040-5809(71)90014-1)

Kimura M, Ohta T. 1971. Theoretical Aspects of Population Genetics. Princeton University Press, Princeton, N.J.

Kong A et al. 2002. A high-resolution recombination map of the human genome. *Nat Genet.* 31(3):241–247. <https://doi.org/10.1038/ng917>

Lande R. 1976. Natural selection and random genetic drift in phenotypic evolution. *Evolution.* 30(2):314–334. <https://doi.org/10.2307/2407703>

Langley CH et al. 1988. On the role of unequal exchange in the containment of transposable element copy number. *Genet Res.* 52(3):223–235. <https://doi.org/10.1017/s0016672300027695>

Li N, Stephens M. 2003. Modeling linkage disequilibrium and identifying recombination hotspots using single-nucleotide polymorphism data. *Genetics.* 165(4):2213–2233. <https://doi.org/10.1093/genetics/165.4.2213>

Marsh JI, Kaushik S, Johri P. 2026. Effects of rescaling forward-in-time population genetic simulations. *Genetics.* iyaf263. <https://doi.org/10.1093/genetics/iyaf263>

Masaki N, Browning SR. 2025. Modeling the length distribution of gene conversion tracts in humans from the UK Biobank sequence data. *PLOS Genet.* 21(11):e1011951. <https://doi.org/10.1371/journal.pgen.1011951>

Morton NE, Crow JF, Muller HJ. 1956. An estimate of the mutational damage in man from data on consanguineous marriages. *Proc Natl Acad Sci U S A.* 42(11):855–863. <https://doi.org/10.1073/pnas.42.11.855>

Nei M. 1968. The frequency distribution of lethal chromosomes in finite populations. *Proc Natl Acad Sci.* 60(2):517–524. <https://doi.org/10.1073/pnas.60.2.517>

Nelson D et al. 2020. Accounting for long-range correlations in genome-wide simulations of large cohorts. *PLOS Genet.* 16(5):e1008619. <https://doi.org/10.1371/journal.pgen.1008619>

Nordborg M. 1997. Structured coalescent processes on different time scales. *Genetics.* 146(4):1501–1514. <https://doi.org/10.1093/genetics/146.4.1501>

Ohta T, Kimura M. 1971. Linkage disequilibrium between two segregating nucleotide sites under the steady flux of mutations in a finite population. *Genetics.* 68(4):571–580. <https://doi.org/10.1093/genetics/68.4.571>

Olito C, Abbott JK. 2025. The evolution of suppressed recombination between sex chromosomes and the lengths of evolutionary strata. *Evolution.* 79(7):1371–1385. <https://doi.org/10.1093/evolut/qpaf045>

Ollivier L, Charlesworth B, Pouyet F. 2025. Beyond recombination: Exploring the impact of meiotic frequency on genome-wide genetic diversity. *PLOS Genet.* 21(8):e1011798. <https://doi.org/10.1371/journal.pgen.1011798>

Otto SP, Payseur BA. 2019. Crossover interference: Shedding light on the evolution of recombination. *Annu Rev Genet.* 53:19–44. <https://doi.org/10.1146/annurev-genet-040119-093957>

Owen ARG. 1953. Super-recombination in the sex chromosome of the mouse. *Heredity*. 7:103–110. <https://doi.org/10.1038/hdy.1953.10>

Pollak E. 1987. On the theory of partially inbreeding populations. I. Partial selfing. *Genetics*. 117:353–360. <https://doi.org/doi:10.1093/genetics/117.2.353>

Rasmussen MD, Hubisz MJ, Gronau I, Siepel A. 2014. Genome-wide inference of ancestral recombination graphs. *PLOS Genet*. 10(5):e1004342. <https://doi.org/10.1371/journal.pgen.1004342>

Robbins RB. 1918. Some applications of mathematics to breeding problems III. *Genetics*. 3(4):375–389. <https://doi.org/10.1093/genetics/3.4.375>

Robertson A. 1960. A theory of limits in artificial selection. *Proc R Soc B*. 153(951):234–249. <https://doi.org/10.1098/rspb.1960.0099>

Robertson A. 1970. A theory of limits in artificial selection with many linked loci. In: Kojima K, editor. *Mathematical Topics in Population Genetics*. Springer-Verlag, Berlin, Heidelberg; p 246–288. https://doi.org/10.1007/978-3-642-46244-3_8

Robinson JA et al. 2022. The critically endangered vaquita is not doomed to extinction by inbreeding depression. *Science*. 376(6593):635–639. <https://doi.org/10.1126/science.abm1742>

Sarens M, Copenhaver GP, De Strome N. 2021. The role of chromatid interference in determining meiotic crossover patterns. *Front Plant Sci*. 12:656691. <https://doi.org/10.3389/fpls.2021.656691>

Schaal SM, Haller BC, Lotterhos KE. 2022. Inversion invasions: when the genetic basis of local adaptation is concentrated within inversions in the face of gene flow. *Philos Trans R Soc B Biol Sci*. 377(1856):20210200. <https://doi.org/10.1098/rstb.2021.0200>

Schrempf D, Minh BQ, von Haeseler A, Kosiol C. 2019. Polymorphism-aware species trees with advanced mutation models, bootstrap, and rate heterogeneity. *Mol Biol Evol*. 36(6):1294–1301. <https://doi.org/10.1093/molbev/msz043>

Speidel L et al. 2021. Inferring population histories for ancient genomes using genome-wide genealogies. *Mol Biol Evol*. 38(9):3497–3511. <https://doi.org/10.1093/molbev/msab174>

Speidel L, Forest M, Shi S, Myers SR. 2019. A method for genome-wide genealogy estimation for thousands of samples. *Nat Genet*. 51(9):1321–1329. <https://doi.org/10.1038/s41588-019-0484-x>

Spence JP, Zeng T, Mostafavi H, Pritchard JK. 2023. Scaling the discrete-time Wright–Fisher model to biobank-scale datasets. *Genetics*. 225(3):iyad168. <https://doi.org/10.1093/genetics/iyad168>

Stephan W, John S. 2020. Polygenic adaptation in a population of finite size. *Entropy*. 22(8):907. <https://doi.org/10.3390/e22080907>

Thornton KR. 2014. A C++ template library for efficient forward-time population genetic simulation of large populations. *Genetics*. 198(1):157–166.
<https://doi.org/10.1534/genetics.114.165019>

Thornton KR. 2019. Polygenic adaptation to an environmental shift: temporal dynamics of variation under gaussian stabilizing selection and additive effects on a single trait. *Genetics*. 213(4):1513–1530. <https://doi.org/10.1534/genetics.119.302662>

Wakeley J. 2008. *Coalescent Theory. An Introduction*. Roberts and Company, Greenwood Village, CO.

Walsh B, Lynch M. 2018. *Evolution and Selection of Quantitative Traits*. Oxford University Press.

Williams AL et al. 2015. Non-crossover gene conversions show strong GC bias and unexpected clustering in humans. *eLife*. 4:e04637. <https://doi.org/10.7554/eLife.04637>

Wohns AW et al. 2022. A unified genealogy of modern and ancient genomes. *Science*. 375(6583):eabi8264. <https://doi.org/10.1126/science.abi8264>

Wright S. 1931. Evolution in Mendelian populations. *Genetics*. 16(2):97–159.
<https://doi.org/10.1093/genetics/16.2.97>

Wright S. 1935. The analysis of variance and the correlations between relatives with respect to deviations from an optimum. *J Genet*. 30(2):243–256. <https://doi.org/10.1007/BF02982239>

Zhao H, Speed TP, McPeek MS. 1995. Statistical analysis of crossover interference using the chi-square model. *Genetics*. 139(2):1045–1056. <https://doi.org/10.1093/genetics/139.2.1045>

Živković D, Steinrücken M, Song YS, Stephan W. 2015. Transition densities and sample frequency spectra of diffusion processes with selection and variable population size. *Genetics*. 200(2):601–617. <https://doi.org/10.1534/genetics.115.175265>

APPENDIX

1. The rate of substitution of mutations

Let N_H be the number of haploid genomes among breeding adults in a discrete-generation model ($N_H = 2N$ in the case of an autosomal locus). The rate of substitution of mutations, K , is equal to the product of the rate of input of new mutations (N_{HU}) and their probability of fixation, denoted here by $Q(q_0)$, where $q_0 = 1/(N_H)$ for a new mutation represented by a single copy. Diffusion theory provides the following general formula for $Q(q_0)$ (Ewens 2004, p.140):

$$Q(q_0) = \frac{\int_0^{q_0} \psi(y) dy}{\int_0^1 \psi(y) dy} \quad (\text{A1a})$$

where $\psi(y)$ is independent of q_0 and is defined as the following indefinite integral:

$$\psi(y) = \exp -2 \int \frac{M_{\delta y}}{V_{\delta y}} dy \quad (\text{A1b})$$

In general, K is *not* given by the product of N_{Hu} and a quantity that is either independent of N or proportional to $1/N_H$. If the former property applied, no rescaling would be needed to obtain the value of K for the natural population, since the product of rescaled N_H and u is independent of population size; in the latter case, the value for the natural population in units of generations could be obtained by dividing the simulation value by C . For selection on an autosomal locus, as described by Equation (2), Equations (A1) give the following results:

$$\psi(y) = \exp \left\{ -4N_e s \left[hy + \frac{1}{2}(1-2h)y^2 \right] \right\} \quad (\text{A2a})$$

where $s > 0$ for a favorable mutation and $s < 0$ for a deleterious one.

If $h = \frac{1}{2}$ (a semi-dominant allele), Equation (A1a) simplifies to the widely-used result of Kimura (1964):

$$Q \left(\frac{1}{2N} \right) = \frac{\left[1 - \exp \left(-\frac{N_e s}{N} \right) \right]}{\left[1 - \exp(-2N_e s) \right]} \approx \frac{\frac{N_e s}{N}}{\left[1 - \exp(-2N_e s) \right]} \quad (\text{A2b})$$

Provided that N_e and N for the simulated population are divided by the scaling factor C and s is multiplied by C , this result implies that Q for the simulated population is greater than that for the natural population by a factor of C , provided that s is sufficiently small that the approximation for Q is accurate. The rate of substitution for favorable mutations is then approximated by:

$$K = 2Nu Q \left(\frac{1}{2N} \right) \approx 2N_e us \quad (\text{A3})$$

If u is scaled by multiplication by C , K is unaffected by the rescaling, provided that time is measured in units of $2N_e$ generations, or if the rate of substitution obtained from the simulation is divided by C to obtain the natural population value of K in time units of generations. Another way of looking at this result is that K relative to the neutral substitution rate u is independent of the scaling factor; the same applies to the ratio of Q and the neutral fixation probability $1/(2N)$.

It is not obvious whether this type of result holds for all values of h , due to the quadratic term in y in Equation (A2a). For a completely recessive, favorable mutation ($h = 0, s > 0$), however, the following approximation for Q is valid (Kimura 1964, Equation 10.13):

$$Q\left(\frac{1}{2N}\right) \approx \left(\frac{N_e}{N}\right) \sqrt{\frac{2s}{\pi N_e}} \quad (\text{A4})$$

With a scaling factor of $1/C$ for N_e and C for s , Q is multiplied by C , just as in the semidominant case, so that the same scaling principles apply.

The situation for deleterious recessive mutations or mutations with h values other than 0 or $1/2$ can be clarified by using the more general selection equation in which h in Equation (2) is replaced by a constant a and $(1-2h)$ by a constant b . This formulation can be used to describe many different scenarios, including inbreeding and sex-linkage, if $2N$ is replaced by N_H , the number of haploid genomes among breeding adults (Charlesworth 2022), so that $q_0 = 1/N_H$ for a new mutation. We can then write the indefinite integral of $\psi(y)$ in Equation (A1b) as follows (correcting a misprint in Equation A3a of Charlesworth (2022)):

$$\int \psi(y) dy = y + \sum_{i=1}^{\infty} \frac{(-\gamma)^i}{i!} \int (2ay + by^2)^i dy \quad (\text{A5})$$

where $\gamma = 2N_e s$.

The definite integral in the numerator of Equation (A1a) can be written as:

$$\int_0^{q_0} \psi(y) dy = \frac{1}{N_H} \left\{ 1 - \frac{\gamma}{N_H} \left[a + \frac{b}{3N_H} \right] + O\left(\left[\frac{\gamma}{N_H}\right]^2\right) \right\} \quad (\text{A6a})$$

If $N_H \gg 1$ and N_e and N_H are of similar magnitude, we have:

$$\int_0^{q_0} \psi(y) dy \approx \frac{1}{N_H} \left(1 - \frac{a\gamma}{N_H} \right) \quad (\text{A6b})$$

The term inside the brackets can be neglected if s is sufficiently small. The denominator in Equation (A1a) involves the sum of 1 and successive powers of γ (see Equation A4b of Charlesworth 2022) and is thus independent of the scaling factor if N_{es} is fixed. It thus follows that, to a good approximation, the ratio of the fixation probability to $1/N_H$ is also independent of the scaling factor, just as in the two limiting cases described above. There should thus be no difficulty in using a simulation of a small population to predict the rates of substitution in a large population, provided that the selection coefficient in the small population is sufficiently small that second-order terms in s can be neglected. This is consistent with the results of Johri et al. (2021) where Drosophila-like populations were scaled by $C = 200$.

2. Times to loss and fixation

Some other quantities that depend on the initial conditions do not, however, have this desirable property, notably the expected time to loss of a new mutation conditional on its loss measured relative to $2N_e$, denoted by t^{**} . To establish this point, it is sufficient to use the following approximation, valid for γ of order 1 (Charlesworth 2022, Equation 3):

$$t^{**} \approx 2N_H^{-1} \{ \ln(N_H) - 1 - \frac{5}{18}\gamma b - \frac{1}{18}\gamma^2 [a(5a + \frac{7}{2}b) + \frac{17}{100}b^2] \} \quad (\text{A7})$$

Even in the neutral case, for which $t^{**} = 2N_H^{-1}[\ln(N_H) - 1]$, the dependence on N_H cannot be scaled out, because of the term $\ln(N_H)$. In contrast, the neutral expected conditional time to fixation relative to $2N_e$, is simply $t^* = 2$.

The result for t^{**} implies that the equilibrium expected number of segregating nucleotide sites (denoted by S) for a sequence of length L is also non-scaleable, assuming the infinite sites model (Kimura 1971), as can be seen as follows. Under this model, S is assumed to be very small compared with L , so that each new mutation can be assumed to arise at a fixed site. S is then

given by the product of $2N_e$, the rate of input of mutations $N_{Hu}L$, and the expected sojourn time of a mutation in the population relative to $2N_e$ (Ewens 2004, p.298). The latter is equal to:

$$t = Q \left(\frac{1}{N_H} \right) t^* + [1 - Q \left(\frac{1}{N_H} \right)] t^{**} \quad (\text{A8})$$

In the neutral case, with $Q = 1/N_H$, we obtain the expression:

$$S \approx 4N_e u L \ln(N_H) \quad (\text{A9a})$$

A more accurate expression (Ewens 2004, p. 298), which corrects for the inaccuracy involved in equating integration and summation and for slight deviations from the predictions of the diffusion approximation, is:

$$S \approx 4N_e u L [\ln(N_H) + 0.6775] \quad (\text{A9b})$$

S is clearly dependent on N_H in a manner that cannot be rescaled. The same applies to the distribution of allele frequencies at segregating sites (the site frequency spectrum or SFS), as can be seen as follows. The expected numbers of sites with derived variants at specified frequencies provides a substitute for a probability distribution (Kimura 1971). If $t(q, q_0)$ is the density function for the time (in units of $2N_e$ generations) that a mutation spends at frequency q given an initial frequency q_0 , and N_{Hu} is the rate at which mutations enter the population, the expected number of segregating sites out of L sites that have variants at between frequencies q and $q + dq$ is $2N_H N_e L u t(q, q_0) dq$, with $q_0 = 1/N_H$ (Ewens 2004, pp.198-199).

We can represent the SFS for the population in terms of the fraction of sites at frequency q (where $q = 1/N_H$ to $q = 1 - 1/N_H$ in steps of $1/N_H$) among all segregating sites, noting that the factor $2N_H N_e L u$ cancels from top and bottom:

$$\phi(q, q_0) = \frac{t(q, q_0)}{\sum t(q, q_0)} \quad (\text{A10a})$$

In general, therefore, the SFS for the population is dependent on N_H . For example, in the neutral case, it is found that $t(q_0) \approx 2N_H^{-1}q^{-1}$ and $\sum t(q, q_0) \approx 2N_H^{-1}[\ln(N_H) + 0.6775]$ (Ewens 2004, p.177) so that (with $q_0 = 1/N_H$) we have:

$$\phi(q, q_0) = \frac{1}{q[\ln(N_H) + 0.6775]} \quad (\text{A10b})$$

The ratios of $\phi(q, q_0)$ for different q values are, however, independent of N_H , as the denominator of this expression is separable into two components, one of which depends only on N_H and the other only on q .

3. Properties of samples from populations

In contrast to the results for the whole population, the properties of samples from populations at statistical equilibrium are scaleable, given certain assumptions. Under the infinite sites neutral model, the SFS for a sample of n alleles can be found as follows. The probability of observing i copies of the derived variant when N_H is large is proportional to:

$$\frac{n!}{i!(n-i)!} \int_0^1 q^{i-1} (1-q)^{n-i} dq \approx \frac{n!}{i!(n-i)!} B(n+1, i) = \frac{1}{i} \quad (\text{A11a})$$

where $B(n+1, i)$ is the beta function, $(n-i)!/[(i-1)!n!]$.

To obtain the SFS among segregating sites, we have to normalize by dividing by the sum of the harmonic series $1/i$ from $i = 1$ to $n - 1$, *i.e.* Watterson's correction factor a_n , giving the sample SFS as:

$$P_i = \frac{1}{ia_n} \quad (\text{A11b})$$

In general, if the population SFS is separable into two components, one of which is a function only of q and the other only of N_H , as in the neutral case, the same lack of dependence of the sample SFS on N_H should hold. This is always the case for single-locus selection models, as can be seen as follows. Equation (A8) of Charlesworth (2022) shows that $t(q, q_0)$ with $q_0 = 1/N_H$ depends on N_H through a factor of N_H that multiplies terms that are a function of q and the scaled selection coefficient γ . If $t(q, q_0)$ is integrated or summed over the interval $(N_H^{-1}, 1 -$

N_H^{-1}), there will be a dependence on N_H for the population SFS, as in Equation (A10a). However, if the SFS is determined from the integral of the product of $t(q, q_0)$ and the binomial sampling formula for i copies of the mutant allele, conditioned on q , the normalization of the type used for Equations (A11) means that there is no dependence on N_H in the final expression. Thus, while the population SFS is not scaleable, the sample SFS for derived variants and statistics based on these (e.g. Tajima's D) should be scaleable, at least if the infinite sites assumption holds.

4. Selection on a quantitative trait

A general expression for selection on a single diallelic locus that makes a small contribution to variation in a quantitative trait controlled by many loci with small effects is given by (Bürger 2000, p.201), which is based on earlier work of Fisher (1930, pp. 104-110), Haldane (1930) and Wright (1935). A simplified account is presented here. Consider a single diallelic autosomal locus that affects the trait, and which segregates for alleles A_1 and A_2 with frequencies p and q , respectively. Consider all individuals with trait value z . Let the values of the trait for A_1A_1 , A_1A_2 and A_2A_2 be $z + a$, $z + d$ and $z - a$, respectively. If the alleles are semidominant, $d = 0$. Note that these are the trait values averaged over all genotypes and environments for the generation in question and are thus not necessarily fixed quantities. Assume that a and d are the same for all values of z , which implies an absence of epistatic interactions with respect to other loci affecting the trait, as well as an absence of genotype- environment interactions.

Let $w(z)$ be the mean fitness of individuals with trait value z and \bar{w} be the mean fitness of the population. If a and d are sufficiently small that terms of order a^3 and d^3 can be neglected, the fitnesses of the three genotypes at the locus can be approximated using Taylor's theorem:

$$w_{11} = E\{w(z - a)\} \approx \bar{w} - a E\{w'(z) - \frac{a}{2}w''(z)\} \quad (A12a)$$

$$w_{12} = E\{w(z + d)\} \approx \bar{w} + d E\{w'(z) + \frac{d}{2}w''(z)\} \quad (A12b)$$

$$w_{22} = E\{w(z + a)\} \approx \bar{w} + a E\{w'(z) + \frac{a}{2}w''(z)\} \quad (A12c)$$

where $w'(z)$ and $w''(z)$ are the first and second derivatives of $w(z)$ with respect to z .

Using these expressions, the difference between the marginal fitnesses of A_2 and A_1 , $w_2 = pw_{12} + qw_{22}$ and $w_1 = pw_{11} + qw_{12}$ (Fisher's "average excess" with respect to fitness), is given by:

$$w_2 - w_1 \approx [a + (p - q)d]w' + \frac{1}{2}(q - p)(a^2 - d^2)w'' \quad (\text{A13a})$$

where w' and w'' are the expectations of $w'(z)$ and $w''(z)$, respectively. The change in the frequency of A_2 over one generation is given by:

$$\Delta q = pq(w_2 - w_1)/\bar{w} \quad (\text{A13b})$$

so that $s = (w_2 - w_1)/\bar{w}$ measures the strength and direction of selection on A_2 .

A widely used representation of the relation between phenotype and fitness is to write

$$w(z) = \exp[kf(z)] \quad (\text{A14})$$

where k is a measure of the strength of selection and $f(z)$ describes the shape of the relation between fitness and phenotype. The nor-optimal model used below is a special case of this formula. The use of the exponential function avoids the possibility of negative fitnesses. In this case, we have:

$$w' = k E\{f'(z)w(z)\}, \quad w'' = k E\{[f''(z) + kf'^2(z)]w(z)\} \quad (\text{A15})$$

It is immediately apparent from these expressions that w' is linearly related to k whereas w'' has a quadratic relation, if the expectations are independent of k , which may of course not be the case in general. This implies that it could be hard to find a way to rescale s in Equation (A13b) in such a way as to keep Nes constant, unless selection is sufficiently weak that terms in k^2 can be neglected.

This conclusion can be made more explicit by considering the nor-optimal selection model, with optimal trait value z_0 and inverse measure of selection strength $V_s \equiv 1/2k$:

$$w(z) = \exp \left[-\frac{(z-z_0)^2}{2V_s} \right] \quad (\text{A16})$$

If the trait is normally distributed, this expression yields the well-known expressions for the within-generation changes in mean and variance of z , $\Delta\bar{z}$ and ΔV_z (Lande 1976):

$$\Delta\bar{z} = \frac{V_z(z_0 - \bar{z})}{(V_z + V_s)}, \quad \Delta V_z = -\frac{V_z^2}{(V_z + V_s)} \quad (\text{A17})$$

Substituting $w(z)$ from Equation (A16) into Equations (A15), and using Equations (A17), yields the following results:

$$\frac{w'}{w} = -\frac{1}{V_s} E\{(z - z_0)w(z)\} = \frac{1}{V_s} E\{[z_0 - (\bar{z} + \Delta\bar{z})]w(z)\} = \frac{z_0 - \bar{z}}{(V_z + V_s)} \quad (\text{A18a})$$

$$\frac{w''}{w} = \frac{1}{wV_s} E \left\{ \left[\frac{(z-z_0)^2}{V_s} - 1 \right] w(z) \right\} = \frac{1}{w} E \left\{ \left[\frac{(z-z_0)^2}{V_s^2} \right] w(z) \right\} - \frac{1}{V_s} \quad (\text{A18b})$$

Substitution of these expressions into Equations (A13) shows that, for fixed values of a , d and $z_0 - \bar{z}$, the first term in s is inversely proportional to $V_z + V_s$, whereas the second term has a more complex relation to V_s and $V_z + V_s$. The magnitudes of V_z and \bar{z} reflect the values of the a 's and d 's at the loci affecting the trait, whereas V_s reflects the relation between z and fitness. V_s can be rescaled by C when population size is rescaled by $1/C$, but this does not produce a proportional change even in the first term in the expression for s unless $V_s \gg V_z$, *i.e.*, selection is weak, and the model converges on the quadratic deviations model:

$$w(z) \approx 1 - \frac{(z-z_0)^2}{2V_s} \quad (\text{A19a})$$

In this case, we have

$$w' \approx \frac{(z_0 - \bar{z})}{V_s}, \quad w'' \approx -\frac{1}{V_s} \quad (\text{A.19b})$$

It follows from these relations and Equations (12) that s is now proportional to $1/V_s$ for fixed values of a , d and $z_0 - \bar{z}$, so that rescaling should work with this model, or with the non-optimal model when $V_s \gg V_z$.

Table 1: Population genetic quantities of interest for single-locus models and their properties with rescaling. Note that when rescaling is performed as follows: $N_{\text{scaled}} = N_H/C$, $u_{\text{scaled}} = uC$, $r_{\text{scaled}} = rC$, $m_{\text{scaled}} = mC$, $s_{\text{scaled}} = sC$, and $T_{\text{scaled}} = T/C$, where N_H is the number of haploid genomes among breeding individuals, u is the mutation rate per nucleotide site/generation, r is the rate of recombination per site/generation, and T is an interval of time in generations. Throughout, N_e refers to the effective population size, L to the length of the region, q to the mutant allele frequency, $p=1-q$, and n refers to the sample size.

Population genetic parameter	Theoretical expression	Scaleability
Constants		
Dominance coefficient	h	Does not scale
Selfing probability	S	Does not scale
Properties of mutations		
Probability of fixation of a neutral mutation	$1/N_H$	Proportional to C
Number of fixations of neutral mutations in time T	uT	Preserved with scaling
Expected conditional time to fixation of a neutral mutation	$4N_e$ (see section 2 of Appendix)	Preserved with scaling
Expected conditional time to loss of a neutral mutation	$2N_H[\ln(N_H) - 1]$	Non-linearly related to C
Equilibrium allele frequency of non-recessive strongly deleterious mutations	$\frac{u}{hs}$	Preserved with scaling
Fixation probability (Q) of a new semidominant selected mutation	$Q = \frac{N_e s / N_H}{1 - \exp(-2N_e s)}$	Proportional to $1/C$
Number of fixations of new semidominant selected mutations in time T	$N_H u \times Q \times T$	Preserved with scaling
Expected conditional time to fixation of a new selected mutation	See Equations (A1a) and (A1b) in Charlesworth (2022), where the terms dependent on the initial frequency cancel out in the final expression for t^*	Preserved with scaling
Expected conditional time to loss of a selected mutation	Equation (A7)	Non-linearly related to C

Properties of populations

Variance in fitness between individuals	The variance involves the product of s^2 and a function of the genotype frequencies	Proportional to C^2
Genetic load	Haldane (1937); Crow (1970)	Proportional to C
Inbreeding load	Morton et al. (1956)	Proportional to C

Summary statistics for the entire population

Number of segregating sites under neutrality	$4N_e u L [\ln(N_H) + 0.6775]$	Non-linearly related to C
Expected SFS $[\phi_{neu}(q)]$ of neutral mutations at equilibrium	$\frac{2N_e u}{q}$	Preserved with scaling
Expected SFS of neutral mutations at equilibrium conditional on segregation	$\frac{1}{q \ln(N_H)}$	Non-linearly related to C
Expected SFS $[\phi_{sel}(q)]$ of semidominant selected mutations at equilibrium	$\sim \frac{4N_e u [1 - e^{-2N_e s(1-q)}]}{q(1-q)[1 - e^{-2N_e s}]}$	Preserved with scaling

Summary statistics for a population sample

Number of segregating sites under neutrality	$L \int_0^1 (1 - q^n - p^n) \phi_{neu}(q) dq$	Preserved with scaling
Expected SFS of neutral mutations at equilibrium	$\frac{1}{i}$ <i>i</i> is the allele count in the sample	Preserved with scaling
Expected SFS of neutral mutations at equilibrium conditional on segregation	$\frac{1}{i \sum_{j=1}^{n-1} (\frac{1}{j})}$ <i>i</i> is the allele count in the sample	Preserved with scaling
Expected SFS of semidominant selected mutations at equilibrium	$P_i = \frac{n!}{i! (n-i)!} \int_0^1 q^i p^{n-i} \phi_{sel}(q) dq$	Preserved with scaling
Tajima's D	See section 3 of Appendix	Preserved with scaling
F_{ST}	$\frac{Var(q)}{\bar{q}(1-\bar{q})}$ where $Var(q)$ is the variance in allele frequencies among subpopulations	Preserved with scaling

Table 2: Interference parameters for several species and corresponding recommended maximum lengths of sequences in simulations as a function of the scaling factor C

Organism	Interference Parameter	No. of chrs.	Mean map length	Mean Mb per chr.	Maximum length (Mb)	Source
<i>C. elegans</i>	Complete	6	0.5	28	$28/C$	Hillers et al. (2017)
Mouse*	$m = 10$	20	0.73	135	$81/C$	De Boer et al. (2006); Cox et al. (2009)
Human*	$m = 4$	23	1.55	139	$36/C$	Broman and Weber (2000); Kong et al. (2002)
<i>D. melanogaster</i> **	$m = 4$	5	0.55	24	$17/C$	Zhao et al. (1995); Ashburner et al. (2005)

* This ignores the evidence for a small contribution from non-interfering crossovers.

** These data are for the arms of the 3 major chromosomes; there is no positive crossover interference across the centromere of the two metacentric autosomes.

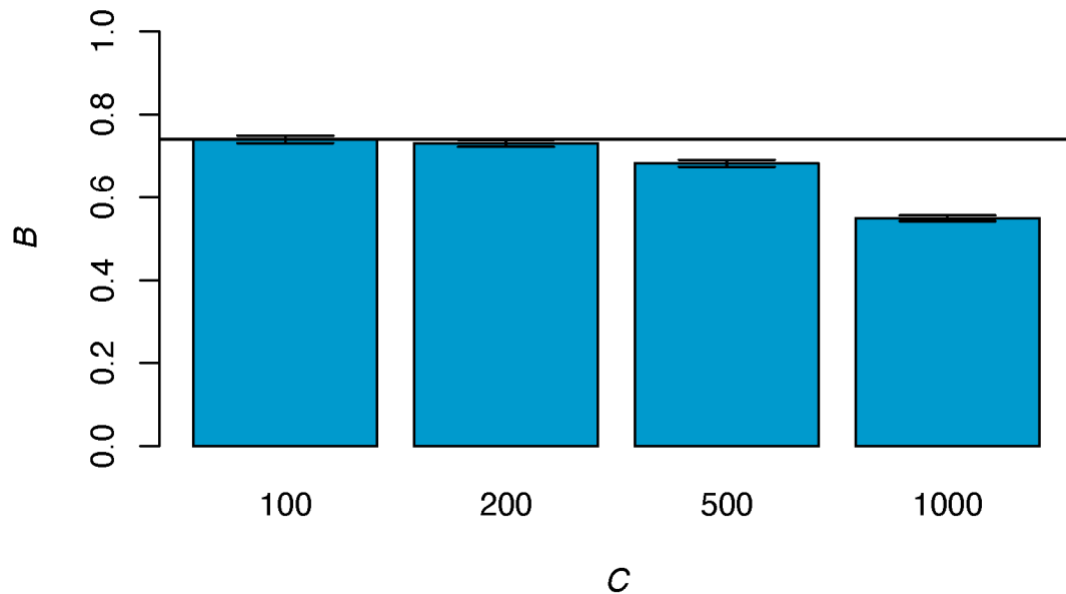


Figure 1: Expected nucleotide diversity (B) at neutral sites in the presence of background selection relative to that under strict neutrality, for different scaling factors (C). The blue bars display mean values and the error bars denote the standard error across 100 independent replicate simulations. Forward-in-time simulations were performed for a 1 Mb region where half of all new mutations were neutral, while the other half experienced purifying selection with a constant selective disadvantage ($2N_{scaled} s = -100$). Selected mutations were uniformly distributed across the simulated region. Simulations mimicked a population of *D. melanogaster* where the Wright-Fisher effective population size before scaling was assumed to be 10^6 , the mutation rate was 3×10^{-9} per site/generation, and the recombination rate was 1×10^{-8} per site/generation. The solid black line represents the infinite population value of $B = \exp(-U/R)$ where U is the genome-wide diploid mutation rate and R is the map length in Morgans, assuming that recombination rate scales linearly with distance. The simulations assumed a lack of crossover interference.

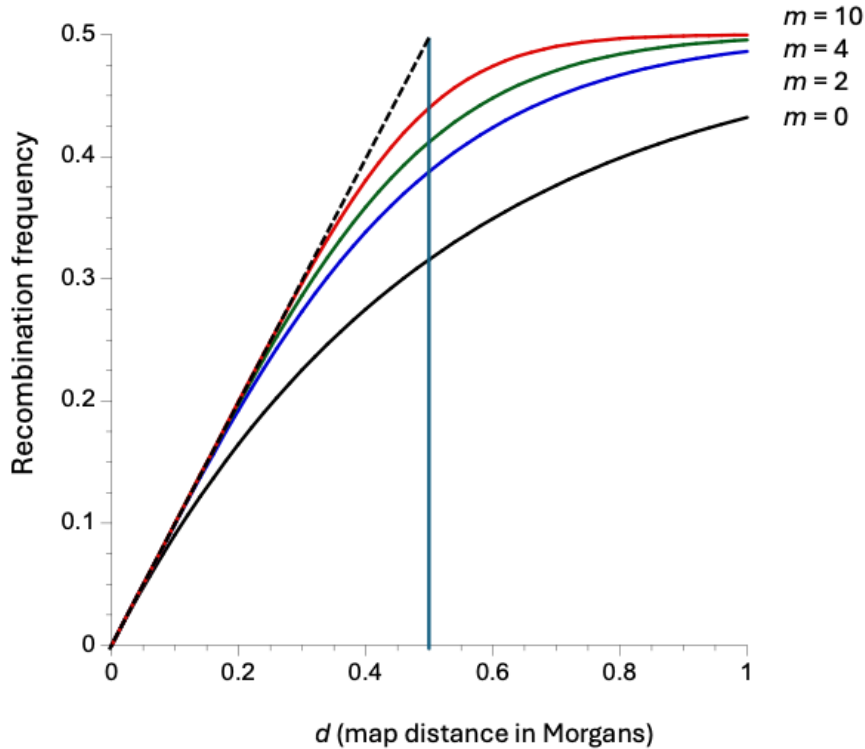


Figure 2: Plots of the recombination frequency between two variants as a function of their map distance in Morgans, for four different levels of interference as predicted by the counting model of Foss *et al.* (1993). The parameter m for each curve is the mean number of non-crossover gene conversion events between successive crossovers, with m increasing from bottom to top. The larger m , the greater the degree of interference between crossovers; $m = 0$ corresponds to the case of no interference (the Haldane mapping function). The vertical line indicates the map distance of $d = 0.5$ Morgans that corresponds to one crossover per bivalent. The dashed line with a slope of 1 indicated the equality of recombination frequency and map distance when there is no interference, with one crossover per bivalent.